TECHNICAL TRANSACTIONS | CZASOPISMO TECHNICZNE
ELECTRICAL ENGINEERING | ELEKTROTECHNIKA

2-E/2016

DOI: 10.4467/2353737XCT.16.244.6043

IRINA.YU. KRUCHININA, ILJA Z. BOGUSLAVSKIY, YUVENALIY PH. KHOZIKOV, ALEXANDR S. LIUBIMTCEV, VALENTINA V. PALTCEVA*

THE CALCULATION APPROACH TO INVESTIGATIONS OF RADIAL MAGNETIC FORCES DUE TO ROTOR ECCENTRICITY

METODYKA OBLICZEŃ W BADANIACH PROMIENIOWYCH SIŁ MAGNETYCZNYCH POWODOWANYCH EKSCENTRYCZNOŚCIĄ WIRNIKA

A b s t r a c t

This paper presents the method of rotor magnetic pulling tensioning force calculation, caused by the static radial rotor eccentricity. The method is applied to calculate the total force acting on the rotor of high-speed permanent magnet (PM) synchronous machine (PMSM). The calculations are based on 2D simulation of magnetic field distribution in the active part of the machine, taking into account the saturation of the magnetic circuit and the spatial harmonics of the air gap magnetic flux in the no-load mode and in the rated mode.

Keywords: rotor eccentricity; high-speed synchronous machines; radial magnetic pulling tensioning forces; permanent magnets

S t r e s z c z e n i e

W artykule przedstawiono metodę obliczania siły naciągu magnetycznego działającej na wirnik, spowodowanej przez radialną ekscentryczność statyczną wirnika. Metoda ta jest stosowana do obliczenia całkowitej siły działającej na wirnik szybkoobrotowej maszyny synchronicznej (PMSM) z magnesami trwałymi (PM). Obliczenia są oparte na symulacji 2D rozkładu pola magnetycznego w aktywnej części maszyny, z uwzględnieniem stopnia nasycenia obwodu magnetycznego oraz harmonicznych przestrzennych strumienia magnetycznego w szczelinie powietrznej w stanie jałowym pracy i dla pracy znamionowej.

Słowa kluczowe: ekscentryczność wirnika; szybkoobrotowe maszyny synchroniczne; promieniowesiły naciągu magnetycznego; magnesy trwałe

* D.Sc.Eng. Irina Yu. Kruchinina, D.Sc. Eng. Ilja Z. Boguslavskiy, Yuvenaliy Ph. Khozikov, Alexandr S. Liubimtcev, Valentina V. Paltceva Institute of Silicate Chemistry named after I.V. Grebenschikov Russian Academy of Sciences (IChS RAS), Federal Agency for Scientific Organizations.

1. Introduction

The rotor eccentricity could be the result of bearing tolerances, bearing wearing or shaft defects. This problem arises both in induction motors [1, 2] and in permanent magnet synchronous motors [3–5]. The rotor eccentricity may increase the load on the bearings. Operation with rotor eccentricity affects the acoustical profile of electrical machine [4, 5].

The trend of recent years [6–9] shows a growing interest in high-speed synchronous machines with permanent-magnet excitation. Such machines are used, for example, in the oil and gas industry (rated power $P = 6–8$ MW and the rotating speed $n > 6000$ rpm), robotic and space technology (rated power $P \leq 1000$ kW, rotating speed $n \leq 60000$ rpm), in modern micro turbine-powered units (gas turbine systems), transport systems of magnetic levitation [3–5, 10–18].

The permanent-magnet synchronous machine operation with radial static rotor eccentricity in no-load and rated modes is studied in this paper.

2. PMSM design specifics

The nine-phase permanent-magnet synchronous generator with rated power of 50 kW and a rotating speed of 15000 rpm has been developed, manufactured and tested at the laboratory of power engineering and chemical energy of IChS RAS some years ago [10, 14]. High-speed permanent-magnet synchronous machines are used in different applications due to their high efficiency, robust construction and compactness as well as reliable excitation. The permanent magnets are fixed on the rotor with non-magnetic sleeves. Usually, machines of this kind are not equipped with a damper winding.

The rotor diameter size (D_{rot}) and consequently the inner diameter of the stator core (D_{inn}) are limited by the mechanical stress in the rotor structural elements. The winding of the stator is usually made with a small number of slots for the pole and the phase ($Q \leq 2$). The value of Q is limited technologically: it is necessary to place Z slots on a small diameter stator; where $Z = 2p \cdot m \cdot Q$; m is the number of phases. In the case of integer Q ($Q = 1$, $Q = 2$), air gap magnetic flux contains a significant portion of tooth harmonics (Carter factor is less than 1.6–1.8). In the case of non-integer $Q \leq 2$, additional "winding" harmonics becomes appears [19, 20]; they are particularly substantial when Q is close to 1. It should be pointed out that recently produced high-speed machines have the stator winding with $Q < 1$. Methods of constructing windings with non-integer $Q > 1$ are laid out in [12], and for $Q \geq 1$ and $Q < 1$ in [21, 22].

Due to certain technological reasons, permanent magnets for high-speed machines are manufactured in a way that the minimal to maximal air gap ratio is $\delta\min/\delta\max = 1$; consequently, the excitation field in addition to the unity harmonic contains a number of higher spatial harmonics. Higher spatial harmonics of magnetic flux cause additional problems associated with added losses and heating of active steel and stator winding as well as vibrations of the stator core.

One of the design problems is the evaluation of the magnetic pulling tensioning forces or magnetic radial forces caused by the rotor eccentricity with the respect to the magnetic flux higher spatial harmonics. An evaluation of these forces is essential for the correct calculation of the magnetic bearing load.

3. Simulation model for the no-load mode

The relative static eccentricity of less than 10% is usually considered acceptable due to the practice of electrical engineering. The eccentricity norm is usually less than 10% for high-speed machines.

Only the unity harmonic magnitude of the magnetic flux density in the air gap is taken into account in the use of the simple analytical method of radial force calculation described in [25]. The flux distribution is determined with the assumption of the smooth air gap in the no-load mode using equation (1a). It is considered that calculations for the no-load mode are sufficient; forces for the rated mode are not usually calculated.

$$b_{calc}(s) = \frac{b_0(s)}{1 - \varepsilon \sin(s)} \tag{1a}$$

where

$b_0(s)$ – magnetic flux density distribution along uniform air gap,

ε – flux density distortion coefficient due to the rotor eccentricity.

s – angular coordinate (0...2π). Coordinate s is measured in clockwise direction from the axis orthogonal to the eccentricity displacement vector.

The distortion coefficient in equation (1a) is in essence the relative eccentricity value, which is calculated as a ratio of the shaft displacement value to the length of the symmetric air gap.

However, in practice, the presence of high-order spatial harmonics in the air gap requires a certain adjustment of known and applied methods of radial forces calculation. It is advisable to use numerical methods to estimate these forces with account to the real distribution of the magnetic flux density in the air gap. The application of computational software packages facilitates the solution to this problem; the solution can be received in a two-dimensional formulation [26] with accuracy sufficient for practical purposes.

Computations are performed in the 2D domain of the cross-section geometry of a synchronous electric machine. Static rotor eccentricity can be characterized by two parameters: by the rotor axis displacement value, and by the angle ψ between the direction of the displacement vector and the Y axis. The origin of a coordinate system coincides with an axis of rotation, the axis (Y) is a vertical (longitudinal stator) axis, and axis (X) is the horizontal (quadrature stator) axis. It is convenient do define parameter ε as the ratio of the rotor displacement value (relative to coordinates origin) to the uniform gap δ length.

The result of FEM simulation is the magnetic flux density distribution. To calculate the magnetic pulling tensioning forces acting on the rotor, the radial component of the flux density and the distribution along the rotor circumference is used. The numerical results of the magnetic flux density are defined in the middle of the air gap (not on the stator/rotor surface) to avoid steel-to-air boundary effects.

Numerical calculations have been performed by dividing the circumference into arc segments Δs_k. The radial component value of magnetic flux density b_{calc} for each segment was measured. The radial magnetic force was calculated using equation (1).

The magnetic flux density can be considered as constant along the air gap length, as the air gap length is much less than the rotor radius. The stator internal circumference (D_{inn}) has been chosen as a reference surface for magnetic force calculation.

$$f_{calc}(s_k) = 0,5\left(\frac{b_{calc}^2(s)}{\mu_0}\right)\Delta s_k L_{ef} \tag{1}$$

where:

- s – angular coordinate (0..2π) of segment Δs_k
- μ_0 – permeability of free space,
- L_{ef} – effective length of the stator core,
- $\Delta s_k = \text{const}$ – length of the arc segment,
- k – index of the segment. It lays between $k = 0$ and $k = k_0 = \dfrac{\pi D_{inn}}{\Delta s_k}$; the segment Δs_k with index $k = 0$ occupies position at the intersection of negative axis (X) with a stator internal circumference D_{inn}.

The analytical approach gives from 5% to 15% overestimation of the resulting magnetic force in the case of low values of the relative eccentricity (less than 0.05). Numerical simulation of the same test case [25] reveals that equation (1a) accuracy could be improved if the relative eccentricity ε as a ratio of the shaft displacement value to the rotor radius is used. This approach is consistent with the principle of virtual work. The difference in distributions of magnetic flux density in the air gap calculated by FEM and (1a) for two cases: $\varepsilon = \Delta_{rot}/\delta$ and $\varepsilon = \Delta_{rot}/R_{rot}$ are presented in Fig. 1 and Fig. 2, respectively.

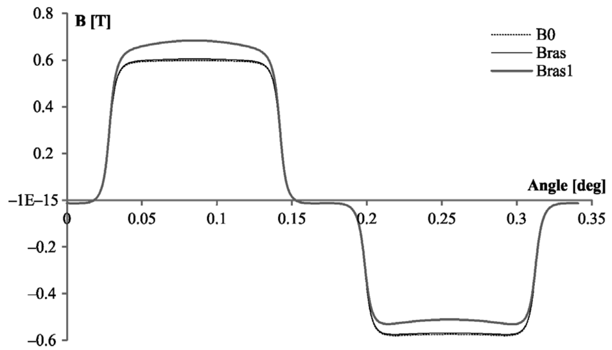

Fig. 1. The distribution of magnetic flux density in the air gap. Relative eccentricity is 0.125 [25]

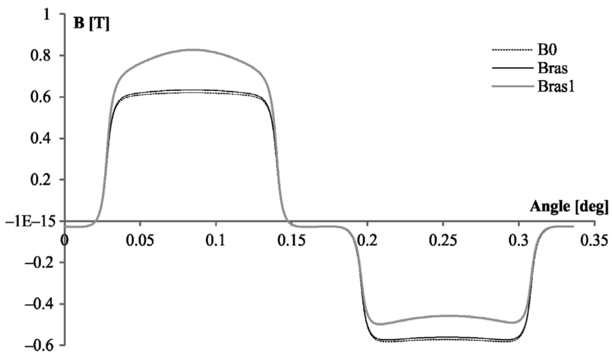

Fig. 2. The distribution of magnetic flux density in the air gap. Relative eccentricity is 0.25 [25]

B0 –magnetic flux density distribution by FEM; B_{ras1} – magnetic flux density distribution by analytical model [25] with $\varepsilon = \Delta_{rot}/\delta$; B_{ras} – magnetic flux density distribution calculated by modified analytical model [25] with $\varepsilon = \Delta_{rot}/R_{rot}$.

As can be seen, if the value of eccentricity is more than 0,1, the calculations are incorrect where $\varepsilon = \Delta_{rot}/\delta$. Thus the magnetic flux density distribution must be calculated by a modified analytical model [25] with $\varepsilon = \Delta_{rot}/R_{rot}$.

The study of bearing load estimation includes:

– the calculation of radial magnetic force distribution $f_{calc}(s_k)$ ($k = 0; 1; 2;\dots; k_0$) in accordance with (1) and calculation of the average radial force applied to the rotor shaft:

$$f_{av}(s_k) = \left(\frac{1}{k_0}\right)\Sigma\left|f_{calc}(s_k)\right| \quad (k = 0;1;2;...;k_0); \tag{2}$$

– the calculation of the resulting bearing force $F_{bear,res}$ and its two components, $F_{bear,1}$ and $F_{bear,2}$:

$$F_{bear,res} = \left|F_{bear,1} - F_{bear,2}\right| \tag{3}$$

$$F_{bear,1} = \Sigma f_{calc}(s_k)\cdot\left|\cos\psi_k\right| \quad (k = 0;1;2;...;k_0)$$

$$F_{bear,2} = \Sigma f_{calc}(s_k)\cdot\left|\cos\psi_k\right| \quad (k = 0,5k_0+1;\ 0,5k_0+2;...;k_0)$$

where:

ψ_k – angle between the midpoint of segment Δs_k and a positive direction of axis (Y).

The rated power, phase voltage and current, rotating speed, frequency, geometric dimensions of the stator active part and its winding parameters as well as nonlinear properties of the magnetic circuit materials are considered to be predefined. The main aim of the investigations is to define the distribution of the radial magnetic force $f_{calc}(s_k)$, the average radial magnetic force $f_{av}(s_k)$ and the resulting bearing force.

The specifics of permanent magnet synchronous generator constriction are the absence of excitation regulation in the rotor magnetic circuit. The study of the load characteristics reveals that if the load current is drops from the rated value to zero (the no-load mode), the generator voltage increases by 10% to 15% (the reason for this moderate increment is that the winding reactance X_{ad} is considerably less than that of the synchronous machines with electromagnetic excitation). The magnitude B_0 of the air gap magnetic flux unity harmonic increases correspondingly, so that $B_0 > B_{L1}$. This results in an increase of the amplitudes of higher spatial harmonics caused by the stator tooth design and the pole shape.

These spatial harmonics do not rotate synchronously with the rotor. However, the absence of damping winding, typical for the machines of this type, does not diminish the effect of these harmonics on the radial magnetic force distribution.

4. The no-load mode results

The test case of a high-speed permanent magnet synchronous motor with static rotor eccentricity of ε = 10% is studied. The generator rated power is 250 kW; synchronous rotating speed is 48000 rpm. The radial magnetic force distribution $f^{*}_{calc}(s_k)$ in no-load mode is presented in Fig. 3. Line A' corresponds to the actual magnetic flux distribution in the air gar calculated by software package [26], and line A corresponds to the unity harmonic of line A' Fourier decomposition.

The average radial force $f^{*}_{calc}\left(s_k\right)$ is not equal to the average unity harmonic magnetic force $f^{(A')}_{calc}\left(s_k\right)$ The ratio is:

$$f^{*}_{calc}\left(s_k\right) = \frac{f^{(A')}_{calc}\left(s_k\right)}{f^{(A)}_{calc}\left(s_k\right)} = 1.119 .$$

That is one of the reasons of analytical method [25] inaccuracy.

Results for the rated mode (lines B and B') are discussed in the section 7.

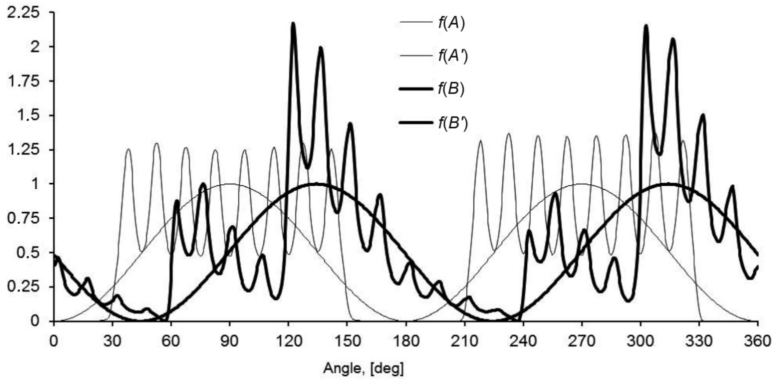

Fig. 3. Distribution of radial magnetic force components in the no-load mode (A, A') and in the rated mode (B, B') for PMSM-0.25-48000

5. Simulation model for the rated mode

The analytical method used to calculate the radial magnetic force acting on the rotor of a synchronous machine in load mode operating with rotor eccentricity does not exists.

Therefore, the evaluation of air gap magnetic flux higher spatial harmonics presents the main difficulty (as compared to the no-load mode). The magnetic field in load mode represents the sum of stator core field and rotor pole field. The magnetic field is distorted as compared to the no-load mode. The resulting magnetic flux is not aligned with rotor pole axis, but shifted on the load angle (Θ). Moreover, the stator winding may induce its own spatial harmonics. The order of these harmonics depends on Q – number of slots per pole and phase.

Evaluation of all range of harmonics in the air gap of the machine operating in the rated mode has been of practical interest (especially for machines with electromagnetic excitation). These harmonics affect the radial magnetic force distribution.

To calculate the forces in the rated mode, one should solve the additional problem of determining the mutual position of the rotor and stator for an arbitrary value of eccentricity ε (including the $\varepsilon = 0$ case). This problem arises both in synchronous machines with electromagnetic excitation and in synchronous machines with permanent magnets on the rotor. The solution method adopted for salient-pole synchronous machines (as they are well studied) is presented in this paper.

The practical implementation of the calculation approach is developed on the basis of results obtained and discussed in the paper on ICEM 2014 [28] where some types of different synchronous machines were modeled and analyzed.

6. Synchronous generator load angle Θ estimation

The algorithm for the determination of the mutual position of the rotor and stator is presented step-by-step. Part of the algorithm is based on the FE package [26].

1. Define the geometry model (computational domain) in the simulation package. The geometry model presents the generator cross-section (2D).
2. To determine the direction and magnitude of the stator magneto-motive force F_{st} (first harmonic), assign some values to the phase currents:

$$I_A = I_{rat} = \text{const};\ \ I_B = -0.5 I_{rat} = \text{const};\ \ I_C = -0.5 I_{rat} = \text{const}. \tag{4}$$

Then, mark the point R on the stator inner circumference that stays from the direction to the middle of the phase zone "*A*" by the angle (+π/2) (in positive angle direction). The vector *OR* on the vector diagram corresponds to the stator magneto-motive force (MMF). The magnitude of the MMF is calculated in the simulation package [26].

3. To determine the direction of the resulting magnetic flux Φ_0 (the first harmonic), mark the point H on the stator inner circumference shifted from the point R by the angle *HOR* = (+γ). The equation to calculate the angle value is included in Appendix. The vector *OH* on the vector diagram corresponds to the resulting magnetic flux.
4. To determine the direction of the rotor magnetic flux Φ_{rot} (the first harmonic) and get more accurate value and position of the vector $\Phi_{0,}$ one should perform the following iterative process:
   - Mark the point $M^{(K)}$ on the stator inner circumference shifted from the point H by the angle $HOM = (+\Theta^{(K)})$, where K – is the iteration index. In the geometry model [26], rotate the rotor so that the axis d direction is aligned with the vector *OM*.
   - Apply stator winding phase currents I_A; I_B; I_C and rotor magneto-motive force F_{rot} (in PM synchronous machines the magneto-motive force is calculated according to [29], taking into account permanent magnet demagnetization curve).
   - Calculate the electromagnetic field distribution in the cross-section of synchronous machine. Perform Fourier analysis to get unity harmonic of magnetic flux distribution and the total unity harmonic magnetic flux $\Phi_0^{(K)}$. The flux value Φ_0 should be equal to the one calculated in Appendix a), b), or in other terms – it should correspond to the rated voltage (U_{rat}).
5. Post processing the simulation results.

   5.1. If $\left|\Phi_0^{(K)} - \Phi_0\right| < e_U$ then it is really to quit iterations and to follow to p. 6. The flux value Φ_0 and the load angle Θ are calculated with the required accuracy e_U.

5.2. Else if $\Phi_0^{(K)} > \Phi_0$ then $\Theta^{(K)}$ should be reduced (modify geometry model by rotor rotation by the angle $\Delta\Theta$):

$$\Theta^{(K+1)} = \Theta^{(K)} - \Delta\Theta,$$

where:

$\Delta\Theta$ – is the predefined angle change step.

5.3. If $\Phi_0^{(K)} < \Phi_0$ then $\Theta^{(K)}$ should be increased (modify geometry model by rotor rotation by the angle $\Delta\Theta$):

Then, the simulations (p. 4, p. 5) must be repeated.

6. Recalculation of generator operation mode parameters (including power factor cosφ). Mark the point $H^{(K)}$ on the inner stator circumference that is shifted from the point R by the angle $H^{(K)}OR$. Vector $OH^{(K)}$ on the vector diagram (Fig. 4) corresponds to the resulting magnetic flux $\Phi_0^{(K)}$ (first harmonic). The angle $H^{(K)}OR$ should be equal to the angle HOR, calculated in Appendix. The case $H^{(K)}OR > HOR$ corresponds to over-excitation operation mode of the generator ($\cos\varphi < \cos\varphi_{rat}$), case $H^{(K)}OR < HOR$ corresponds to under-excitation operation mode of the generator ($\cos\varphi > \cos\varphi_{rat}$).

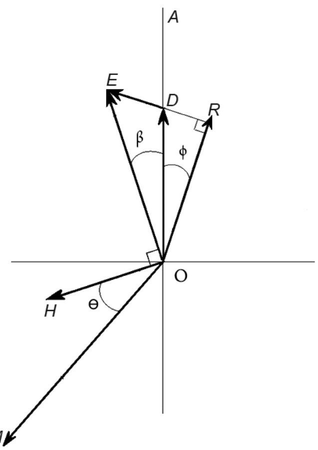

Fig. 4. Vector diagram. See Appendix

The power factor cosφ can be adjusted by excitation current regulation in synchronous machines with electromagnetic excitation. In the case of PM synchronous machines, the power factor cosφ can be adjusted by replacing permanent magnets with other ones that have a new coercive force value.

7. The rated mode results

The radial force distribution $f_{calc}(s_k)$ calculated for the test-case PMSM-0.25-48000 at the rated mode is presented in the Fig. 3. Line B' corresponds to the actual magnetic flux distribution in the air gar calculated by software package [26], and line B corresponds to the unity harmonic of line B' Fourier decomposition. Again, the ratio of the average radial force to the average unity harmonic magnetic force is calculated as:

$$f_{av}^{*}\left(s_k\right)=\frac{f_{calc}^{(B')}\left(s_k\right)}{f_{calc}^{(B)}\left(s_k\right)}=1.120;$$

In addition, a similar ratio for the total force acting on the bearing can be calculated as:

That yields to $F_{bear,res}^{*}=\dfrac{F_{bear,res}^{(B')}}{F_{bear,res}^{(A')}}=0.8;\ \dfrac{f_{av}^{(B')}\left(s_k\right)}{f_{av}^{(A')}\left(s_k\right)}=0.84.$

These results indicate the change in the radial force applied to the bearing in no-load and at rated mode.

8. Appendix

The voltage and current sinusoidal waveform distortion should be limited according to IEC [27] specification. To meet this requirement and reduce higher spatial harmonics, the design of generators provides additional measures, such as skewed stator slots (per one tooth pitch in the axial direction) or a pole shift (single or group) in the tangential direction [19, 20, 22]. This yields to an almost sinusoidal shape of the voltage. Therefore, the phase angle (φ) is defined by the first harmonics of voltage and current.

The relations between unity harmonic of magnetic flux, corresponding magneto-motive force (MMF) and phase voltage are estimated by well-known equations of a synchronous machine [19–20, 28]. These equations determine the electromagnetic loads of a synchronous machine and the power factor ($\cos\varphi_{rat}$) at the rated power mode (P_{rat}). Fig. 4 presents vector diagram illustrating these equations.

a) The relation between stator winding electromotive force (EMF) E and the rated phase voltage (vector OD) is evaluated by the following equation:

$$E=U_{rat}\left[\cos^2\varphi+\left(X_L+\sin\varphi_{rat}\right)^2\right]^{0.5},$$

where:

X_L – stator winding leakage reactance (in relative units).

b) The relation between first harmonic of the air gap magnetic flux Φ_0 (vector OH) and generator electromotive force E (vector OE) is evaluated by the following equation:

$$\Phi_0=\frac{E}{2\pi f w_{st} K_w}$$

where:

f – frequency,
w_{st} – number of turns in the stator phase winding,
K_w – winding factor.

c) Angles on the vector diagram:

$$\angle DOR = \arccos\varphi_{rat}; \ \angle EOD = \beta = \text{ar}\,\text{ctg}\frac{X_L I_{rat}\cos\varphi}{U_{rat}}; \ \angle HOE = 0.5\pi;$$

$$\angle HOM = \Theta; \ \angle HOR = \gamma = \angle DOR + \angle EOD + \angle HOE = \varphi_{rat} + \beta + 0.5\pi.$$

9. Conclusions

The calculation approach has been developed for the calculation of radial magnetic forces due to rotor eccentricity based on FEM at the no-load and the rated modes.

To identify the load angle, it is necessary to simulate the rated mode. The machine magnetic circuit saturation and the higher spatial harmonics of a mutual field of magnetic flux density are considered in both modes.

The magnetic flux is distorted by the stator reaction field at the rated mode. The additional higher spatial harmonics to the magnetic flux spectrum appeared and the magnetic forces distribution changed. The load angle is calculated using graphical options of the simulation package.

The paper describes the practical implementation of the algorithm. The results are obtained for different operating conditions and include differential and integral parameters of the radial magnetic pulling tensioning forces.

Acknowledgments

The authors would like to thank the Russian Foundation for Basic Research for support of the project under Grant 14-08-00817.

References

[1] Dorrell D.G., Hsieh Min-Fu, *Calculation of radial forces in cage induction motors at start – the effect of rotor differential*, IEEE Trans. Magn., vol. 46, no. 8, Aug. 2010, 3029–3032.

[2] Dorrell D.G., *Sources and Characteristics of Unbalanced Magnetic Pull in 3-Phase Cage Induction Motors with Axial-Varying Rotor Eccentricity*, IEEE Trans. Ind. Appl., vol. 47, no. 1, Jan./Feb. 2011, 12–24.

[3] Rezig A., Mekideche M.R., *Effect of rotor eccentricity faults on noise generation in permanent magnet synchronous motors*, Progress in Electromagnetics Research C, vol. 15, 2010, 117–132.

[4] Ebrahimi B., Faiz J., *Diagnosis and performance analysis of three-phase permanent magnet synchronous motors with static, dynamic and mixed eccentricity*, Electric Power Appl., IET 4, vol. 1, Jan. 2010, 53–66.

[5] Torregrossa D., Khoobroo A., Fahimi B., *Prediction of Acoustic Noise and Torque Pulsation in PM Synchronous Machines with Static Eccentricity and Partial Demagnetization Using Field Reconstruction Method*, IEEE Trans. Ind. Electronics, vol. 59, no. 2, Feb. 2012, 934–944.

[6] Mecrow B.C., Jack A.G., *Efficiency trends in electric machines and drives*, Energy Policy, vol. 36, no. 12, 2008, 4336–4341.

[7] Dutta R., Rahman M.F., *Design and analysis of an interior permanent magnet (IPM) machine with very wide constant power operation range*, IEEE Trans. Energy Conv., vol. 23, no. 1, Mar. 2008, 25–33.

[8] Pyrhonen J., Nerg J., Kurronen P., Laube U., *High–Speed, 8 MW, Solid–Rotor Induction Motor for Gas Compression*, Proc. 2008 of XVIII International Conference on Electrical Machines. Paper ID 814.

[9] Nagrial M., Rizk J., Hellany A., *Design and Performance of Permanent Magnet Slotless Machines*, in Proc. 2008 of XVIII International Conference on Electrical Machines, Paper ID 1503.

[10] Kruchinina I., Antipov V., Ivanova A., Khozikov Yu., *Design considerations of high-speed permanent magnet machines for decentralized electro engineering. Evaluating approach*, Proc. of IEEE 2009 International Conference devoted to the 150-annivesary of Alexander S. Popov, 2009, 156–161.

[11] Gieras J.F., Jonsson U., *Design of a High–Speed Magnet Brushless Generator for Microturbines*, in Book of digests 2004 of XVI International Conference on electrical Machines, 363.

[12] Nagorny A., Dravid N.V., Jansen R.H., Kenny B.H., *Design aspects of a high-speed permanent magnet synchronous motor. Generation for flywheel application*, Proc. 2005 of International Electric Machines and Drives Conference. NASA/TM=2005–213651.

[13] Sawada K., *Development of magnetically levitated high speed transport system in Japan*, IEEE Trans. Magn., vol. 32, no. 4, Part 1, 2006, 1917–1925.

[14] Danilevich Y.B., Antipov V.N. , *High–speed (3000–15000 rpm) permanent magnet generator (design and testing)*, Book of Abstracts 2006 ICEM XVII International Conference on Electrical Machines, 2–5.

[15] Danilevich J.B., Antipov V.N., Kruchinina I. Yu., *Finite element analysis and comparison parameters of permanent magnet synchronous and two-ply solid rotor induction motors*, Przegląd Elektrotechniczny, no. 5, 2010, 133–136.

[16] Danilevich J.B., Kruchinina I. Yu., Antipov V.N., Khozikov Y. Ph., Ivanova A.V., *Some Problems of the High Speed Permanent Magnet Miniturbogenerators Development*, Proc. 2008 of XVIII International Conference on Electrical Machines, Paper ID 942.

[17] Danilevich J.B., Kruchinina I. Yu., Antipov V.N., Khozikov Y. Ph., Ivanova A.V., *Prospective Permanent Magnet Turbogenerator Design for Local Power Engineering*, Proc. 2010 of XIX International Conference on Electrical Machines, Paper No. 003603.

[18] Danilevich Y.B., Antipov V., Kruchinina I., *Perspective electromechanical energy converters based on new materials and coatings*, Russian Electrical Engineering, no. 9, Sept. 2010, 2–9.

[19] Mueller G., Ponick B., *Grundlagen elektrischer Maschinen*, J. Willey, 2005, 682.

[20] Mueller G., Vogt K., Ponick B., *Berechnung elektrischer Maschinen*, J. Willey, 2012.
[21] Boguslavskiy I.Z., Kus H., *The investigations of multiphase stator winding structure with fractional number Q*, Electrical Engineering, No. 1, 2000.
[22] Arseniev I.A., Boguslawsky I.Z., Korovkin N.V., *Research Method for the Slot-Ripple EFM in Polyphase Integral Slot Winding*, in Proc. 2012 of the IEEE Russia North West Section, vol. 4, 36–45.
[23] Danilevich Ya.B., Kruchinina I. Yu., Shtainle L. Yu., *Metod raschyota harmonik v zazore electricheskih mashin*// Nauchno-tekhnicheskiye vedomosti SPbGPU. 2011. № 117. S. 221–226. – SPb.: Izd-vo Politekhn. un-ta. 2011 (in Russian).
[24] Kruchinina I. Yu., Shtainle L. Yu., *Magnetomotive Force of Stator Multiphase Windings with Fractional Number of Slots Q per Pole and Phase*. //Allerton Press, Inc. Distributed worldwide by Springer, Russian Electrical Engineering, Vol. 81, No. 8, 2010.
[25] Schuisky W., *Berechnung elektrischer Maschinen*, Springer Verlag, 1960.
[26] *ELCUT – finite element analysis system*, Version 6.0. User's guide, 2013. Tor Ltd., Saint Petersburg, Russia, 295 p.
[27] IEC 60 034-1 Rotating electric machinery; ratings and performances.
[28] Boguslavskiy I.Z., Kruchinina I. Yu., Khozikov Yu. Ph., Lyubimtcev A.S., *High-Speed Synchronous Machines: Magnetic Pulling Tensioning Forces Calculation Approach*, Proc. of the XXI International Conference on Electrical Machines (ICEM'2014), Berlin, Sept. 2–5, 2014, P094 GD-004693.
[29] Schweitzer G., Bleuler H., Traxler A., *Active Magnetic Bearings: Basics, Properties and Applications of Active Magnetic Bearings*, ETZ, Zurich 1994.